
fabric-lib: RDMA POINT-TO-POINT COMMUNICATION FOR LLM SYSTEMS

Nandor Licker* Kevin Hu Vladimir Zaytsev Lequn Chen*

ABSTRACT

Emerging Large Language Model (LLM) system patterns, such as disaggregated inference, Mixture-of-Experts (MoE) routing, and asynchronous reinforcement fine-tuning, require flexible point-to-point communication beyond simple collectives. Existing implementations are locked to specific Network Interface Controllers (NICs), hindering integration into inference engines and portability across hardware providers. We present `fabric-lib`, which bridges the functionality of common NICs to expose a uniform interface. `fabric-lib` exposes one-sided `WRITEIMM` operations with a `IMMCOUNTER` primitive for completion notification, without ordering assumptions of network transport, transparently managing multiple NICs per GPU. We demonstrate peak throughput of 400 Gbps on both NVIDIA ConnectX-7 and AWS Elastic Fabric Adapter (EFA). We showcase `fabric-lib` through three production systems: (1) KvCache transfer for disaggregated inference with dynamic scaling, (2) RL weight updates achieving 1.3 seconds for trillion-parameter models, and (3) MoE dispatch/combine implementation exceeding DeepEP decode latency on ConnectX-7, with the first viable latencies on EFA. We demonstrate that our portable point-to-point communication complements collectives while avoiding lock-in. `fabric-lib` is open-sourced at <https://github.com/perplexityai/pplx-garden/>.

1 INTRODUCTION

Mixture-of-Experts (MoE) architectures are becoming the dominant approach for scaling model capacity (Shazeer et al., 2017), while disaggregated inference is emerging as the standard for production serving. (Patel et al., 2024; Zhong et al., 2024; Qin et al., 2025) These new architectures rely on communication patterns that are fundamentally different from traditional collective-based parallelism.

LLM frameworks overwhelmingly rely on collective communication, often through `NCCL` or `torch.distributed`. (NVIDIA, 2015; Li et al., 2020) While collectives excel at static patterns such as tensor or data parallelism (Shoeybi et al., 2020; Sergeev & Balso, 2018; Zhao et al., 2023), they impose constraints unsuitable for emerging workloads: fixed membership prevents dynamic scaling, synchronized initialization adds overhead, and uniform buffer sizes force dense communication even for sparse patterns. While these libraries offer `SEND` and `RECV` primitives for point-to-point communication, they often cannot be effectively composed to achieve viable latency.

High-performance computing has long used primitives

Perplexity AI. *Equal contribution Correspondence to: Lequn Chen <lequn@perplexity.ai>.

(`SEND`, `RECV`, `WRITE`) built on Remote Direct Memory Access (RDMA) for flexible low-latency high-bandwidth transfers (Kalia et al., 2016), yet such primitives are rarely available in LLM frameworks. The key barrier is hardware diversity without uniform abstraction. Cloud providers deploy different RDMA implementations: NVIDIA ConnectX NICs use traditional Reliable Connection (RC) transport with in-order delivery, while AWS Elastic Fabric Adapter (EFA) implements a proprietary Scalable Reliable Datagram (SRD) protocol (Shalev et al., 2020) with out-of-order delivery. Existing solutions suffer from vendor lock-in: *DeepEP* (Zhao et al., 2025) requires GPU-initiated RDMA (IBGDA) (Agostini et al., 2018) provided exclusively by ConnectX, *NVSHMEM* (Langer et al., 2021) exhibits severe performance degradation on EFA and recent libraries like *Mooncake* (Qin et al., 2025) and *NIXL* (NVIDIA, 2025) lack EFA support or remain preliminary. Consequently, there are no viable cross-provider solutions for LLM inference.

We address portability by leveraging the common functionality across heterogeneous RDMA hardware. Our key insight is that both ConnectX and EFA support reliable but unordered delivery: ConnectX RC can ignore ordering, while EFA SRD is inherently unordered. We introduce `fabric-lib`, a portable RDMA communication library. It provides two-sided `SEND/RECV` and one-sided `WRITEIMM` operations with a novel `IMMCOUNTER` primitive for completion notification that does not rely on message ordering.

It exposes a common interface to both ConnectX and EFA, avoiding vendor lock-in. It transparently manages multiple NICs per GPU, essential for EFA where four 100 Gbps NICs must be aggregated to reach 400 Gbps.

We demonstrate `fabric-lib` through production systems addressing the shortcomings of collectives:

KvCache transfer (Section 4): Disaggregated inference with unrestricted prefiler-decoder communication, enabling elastic scaling without synchronized initialization or fixed membership. Production tested on EFA with full CUDA Graph support and low-latency layer-by-layer transfers.

RL weight update (Section 5): Point-to-point approach achieves 1.3-second updates for trillion-parameter models, over $100\times$ faster than existing RL frameworks. (Huang et al., 2025; He et al., 2025) Utilizes full cluster bandwidth by one-sided RDMA WRITE directly from each training GPU to inference GPUs. Pipelined execution overlaps H2D memcopy, weight preparation, and RDMA transfer.

MoE dispatch/combine (Section 6): State-of-the-art decode latency on ConnectX-7, competitive with specialized *DeepEP* kernels despite the use of a host proxy thread. First viable implementation on EFA, relying on parallel token and route transfers to hide device-to-host and network latency.

The systems we present span diverse communication patterns, ranging from paged writes to bulk transfers and coordinated scatter operations, all production-deployed on heterogeneous hardware. Our results demonstrate that point-to-point communication complements collectives for modern LLM workloads, and that portable abstractions can avoid vendor lock-in while retaining performance.

2 BACKGROUND AND RELATED WORK

2.1 Network Technology

RDMA Remote Direct Memory Access (RDMA) is the high-throughput, low-latency backbone of modern ML systems. Presently deployed NICs deliver 400 Gbps bandwidth at sub- μ s latencies. RDMA achieves its performance through a split design: control plane operations initialize the device and set up buffers with operating system involvement, while data plane operations (data transfer and completion polling) bypass the kernel, avoiding system call overheads.

RDMA Operations RDMA provides both two-sided and one-sided operations. Two-sided SEND/RECV operations first post a RECV with a registered memory region, with the sender issuing a SEND, notifying the receiver via a completion queue. One-sided WRITE operations copy local memory to a remote memory region without peer involvement, requiring the remote memory address and key (RKEY). WRITEIMM extends WRITE by delivering a 32-bit

	RC	UC	UD	SRD	<code>fabric-lib</code>
Reliability	✓	✗	✗	✓	✓
Ordering	✓	✗	✗	✗	✗
Connection	✓	✓	✗	✗	✗
SEND/RECV	✓	✓	MTU	✓	✓
WRITEIMM	✓	✓	✗	✓	✓
READ	✓	✗	✗	✓	✗
Atomic	✓	✗	✗	✓	✗

Table 1. Comparison of RDMA transport types

immediate value that also notifies the receiver via the completion queue. While READ and atomic operations are available, their latencies are not suitable for our purposes. (Kalia et al., 2016; Reda et al., 2022)

RDMA Transports The RDMA specification defines three transport protocols: Reliable Connection (RC), Unreliable Connection (UC), and Unreliable Datagram (UD). Table 1 summarizes their capabilities, highlighting `fabric-lib` as the common ground between them.

Cloud RDMA Adapters Beyond the widely-deployed ConnectX series, major cloud providers are deploying their own solutions, such as AWS Elastic Fabric Adapter (EFA), Alibaba Cloud eRDMA and Google Falcon (Alibaba Cloud, 2025; Singhvi et al., 2025). While most are RC-compatible, EFA implements the proprietary SRD protocol, exposed via `libfabric`. (Shalev et al., 2020; OFIWG, 2014) SRD is connectionless and provides reliable but unordered delivery.

2.2 Programming Interface

Collectives ML frameworks predominantly rely on collective communication libraries (e.g., `torch.distributed`, NCCL, MPI) for inter-GPU data exchange. (Li et al., 2020; NVIDIA, 2015; MPI Forum, 2025) While collective operations excel at structured data transfers, (Shoeybi et al., 2020; Sergeev & Balso, 2018; Zhao et al., 2023) their point-to-point capabilities are limited: **(1) Fixed membership** hinders dynamic scaling by requiring advance knowledge of all participants; **(2) Synchronized initialization** mandates global coordination to form “worlds”, blocking independent peer connections; **(3) Operation ordering** requires all participants to agree on operation sequence, necessitating extra synchronization even when NCCL supports concurrent receives; (Hu et al., 2025b) **(4) Shape uniformity** constrains transfer sizes across participants, even for point-to-point.

GPUDirect GPUDirect RDMA enables RDMA NICs to directly access GPU memory over PCIe, eliminating intermediate CPU memory copies. (NVIDIA, 2012) Transfers can be initiated either by the host, or if GPUDirect Async (IBGDA) is available, from the GPU itself to bypass CPU overheads (Agostini et al., 2018). Currently, GPUDirect Async is only supported on ConnectX NICs. Additionally, GPUDirect RDMA enables low-latency host-device memcopy via the GDRCopy library (Shi et al., 2014).

2.3 Related Work

Disaggregated Inference Splitwise, DistServe, and Mooncake are among the earliest works demonstrating the benefits of disaggregated inference architectures by separating the prefill and decode stages of LLM inference to distinct devices. (Patel et al., 2024; Zhong et al., 2024; Qin et al., 2025) Our KvCache transfer use case implements this paradigm by bridging fabric-lib to an inference engine to connect prefill and decode clusters via RDMA.

Point-to-Point Network Libraries NVSHMEM exposes both collective operations as well as flexible point-to-point communication. (Langer et al., 2021) It supports both GPU-initiated (IBGDA) and host-proxy communication (IBRC). However, it suffers from severe performance degradation on EFA. NVIDIA Inference Xfer Library (NIXL) targets P2P communication for LLM inference, built on UCX (NVIDIA, 2025; Shamis et al., 2015). Our production-deployed EFA implementation predates the preliminary EFA support in NIXL (v0.6.1, October 2025). Mooncake also provides an RDMA Transfer Engine, but without support for EFA. Other libraries, such as UCCL (Zhou et al., 2025) and MSCCL++ (Shah et al., 2025), focus on network-layer optimizations for collectives rather than point-to-point.

Distributed KvCache Storage Mooncake Store and DeepSeek 3FS (DeepSeek AI, 2025) provide distributed storage for KvCaches, albeit they currently lack EFA support. We complement these systems by providing portable RDMA primitives suitable for cloud deployments.

Compute-Communication Overlapping Research on overlapping compute with collective communication for LLM kernels (Chang et al., 2024; Zhang et al., 2025; Zheng et al., 2025a;b) is orthogonal to our focus on RDMA primitives, although we do enable background transfers.

LLM Frameworks fabric-lib can be integrated into LLM inference frameworks and kernel libraries, such as vLLM, SGLang, TensorRT-LLM, FlashInfer. (Kwon et al., 2023; Zheng et al., 2024; NVIDIA, 2023; Ye et al., 2025) Our P2P weight update approach can be adopted by reinforcement learning frameworks, such as Slime, OpenRLHF, AReaL, veRL, LlamaRL, NVIDIA Nemo. (Wu et al., 2025; Zhu et al., 2025; Mei et al., 2025; Fu et al., 2025; Sheng et al., 2024; Hu et al., 2025a)

3 TRANSFERENGINE

The *TransferEngine* is the core component of fabric-lib, enabling efficient RDMA-based point-to-point communication by abstracting heterogeneous hardware under a simple protocol. It exposes SEND/RECV operations to implement RPC-like interfaces. For KvCache transfers, it provides paged WRITES for bulk writes. For RL weight transfers,

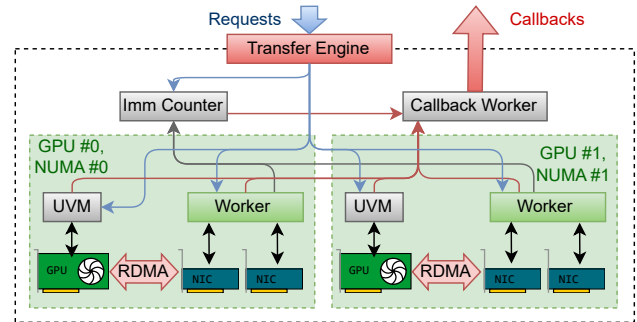


Figure 1. *TransferEngine* managing GPUs across NUMA nodes, each with multiple NICs. Commands are forwarded to workers, which respond back to the callback handler or IMM COUNTER.

it exposes low-latency high-throughput WRITE operations. For MoE routing, it specializes WRITES targeting many peers to implement low-latency SCATTER and BARRIER operations. There are no ordering guarantees across any of the operations. An immediate value can be optionally associated with WRITES to increment a counter on the receiver upon receipt.

The key contributions of the *TransferEngine* are the portable RDMA interface built on reliable-but-unordered transport semantics and the IMM COUNTER primitive for order-agnostic completion notification. The subsections below present the design, API, and engineering optimizations that realize these abstractions.

3.1 Overview and Design Goals

The *TransferEngine* exposes a minimal API that abstracts away the complexity of the underlying RDMA interfaces. It supports multiple interfaces, including EFA with its SRD protocol and a multitude of NICs programmable via libibverbs, including ConnectX-7. Topologies are transparently detected to handle multiple NICs per GPU: while a single ConnectX-7 NIC provides 400 Gbps bandwidth, achieving equivalent bandwidth on AWS p5 instances requires aggregating four 100 Gbps EFA NICs (or two 200 Gbps EFA NICs for p5en instances). A single instance spans multiple threads to manage all GPUs and NICs within a node. Low-latency operations are achieved through zero-copy interfaces and hardware-specific optimizations.

To bridge the gap between the in-order guarantees of RDMA RC and the out-of-order delivery of EFA SRD, the *TransferEngine* relies solely on a novel IMM COUNTER. Instead of relying on ordering guarantees, all completion notifications are handled by polling completion queues and delivering notifications upon the bulk receipt of immediate values. Notifications are delivered through callbacks or atomic flags.

3.2 Architecture

Figure 1 illustrates the architecture of the *TransferEngine*.

```

#[serde] struct NetAddr(Bytes);
#[serde] struct MrDesc{ ptr: u64, rkeys: Vec<NetAddr, u64> }
struct MrHandle(NonNull<c_void>); type Offset = u64;
struct Pages{ indices: Vec<u32>, stride: u64, offset: Offset }
struct PeerGroupHandle(u64);
struct ScatterDst{ len: u64, src: Offset, dst: (MrDesc,Offset)}
enum OnDone { Callback(fn () -> ()), Flag(Atomic<bool>) }

trait TransferEngine {
    fn main_address() -> NetAddr;
    // Memory Region Management
    fn reg_mr(ptr, len, device) -> (MrHandle, MrDesc);
    // Two-sided Send/Recv
    fn submit_send(addr: NetAddr, msg: &[u8], cb: fn () -> ());
    fn submit_recvs(len: u64, cnt: u64, cb: fn (&[u8]) -> ());
    // One-sided Write
    fn expect_imm_count(imm: u32, count: u32, cb: fn () -> ());
    fn submit_single_write(len: u64, imm: Option<u32>
        src: (MrHandle, Offset), dst: (MrDesc, Offset), OnDone);
    fn submit_paged_writes(page_len: u64, imm: Option<u32>,
        src: (MrHandle, Pages), dst: (MrDesc, Pages), OnDone);
    // One-sided Write to a group of peers
    fn add_peer_group(addrs: Vec<NetAddr>) -> PeerGroupHandle;
    fn submit_scatter(h: Option<PeerGroupHandle>, OnDone,
        imm: Option<u32>, src: MrHandle, dst: Vec<ScatterDst>);
    fn submit_barrier(h: Option<PeerGroupHandle>, OnDone,
        imm: u32, dst: Vec<MrDesc>);
    // Watcher for CPU-GPU synchronization
    fn alloc_uvm_watcher(cb: fn(u64,u64) -> ()) -> NonNull<u64>;
}

```

Figure 2. *TransferEngine* API pseudo-code. Error handling, domain sharding, and resource releasing are omitted.

The engine spawns a worker per GPU, with each managing a generic DOMAINGROUP that coordinates all the associated RDMA NICs, typically 1–4 NICs depending on the hardware platform. Within a generic DOMAINGROUP, each DOMAIN is specialized to the hardware and responsible for a single NIC, handling queue pair management, work submission, and completion polling.

Each *TransferEngine* instance exposes a single *main address* for identification and discovery to remote peers. We use a `NetAddr` struct to capture and serialize network address of a DOMAIN, exchanging the structure between peers that wish to communicate. As a restriction, all peers must use the same number of NICs per GPU. Consequently, any transfer has full knowledge of the NICs between the source and destination domain, allowing the *TransferEngine* to shard or balance the request. This is crucial for EFA, which achieves the full 400Gbps bandwidth using multiple adapters.

3.3 API Design

The API exposed by the *TransferEngine* is outlined in Figure 2, implementing the abstractions over RDMA:

Memory Registration Memory regions must be registered with the engine, returning a serializable `MrDesc` that can be exchanged with peers to submit WRITES through and a local `MrHandle` to be used as the source of transfers. The same API can register both host-side buffers and GPU memory. Behind the opaque types, the handles carry the addresses of all the NICs they are associated with, along with the domain-specific remote keys attached to them as a list of (`NetAddr`, `RKEY`) pairs.

Point-to-Point Transfer `submit_send` and its remote counterpart `submit_recvs` wrap the SEND/RECV oper-

ations to expose RPC-style communication, exchanging small payloads. Submission involves a copy to allow the caller to reuse or release the buffer immediately. Receive posts a rotating pool of buffers to receive data into. Upon each message, a buffer is temporarily taken out of the pool to allow the callback to process it without copying. Upon callback completion, it is automatically re-posted. Sufficient buffers must be allocated to avoid rejecting messages. These operations utilize only the first NIC in a domain group.

`submit_single_write` and `submit_paged_writes` transfer data from a source to a destination buffer, writing contiguous or paged regions determined by indirect indices, strides and offsets, respectively. The engine translates these operations into possibly multiple zero-copy one-sided RDMA WRITE operations, sharding and rotating them along the available NICs. Each Transfer can optionally carry a 32-bit immediate number to notify the receiver upon completion. Transfer completion notifications are delivered asynchronously to the caller.

`submit_scatter` send a slice from a source buffer to each peer in a peer group at different offsets in their receive buffers, while `submit_barrier` is an immediate-only operation for peer notification. These are optimized wrappers around WRITE, allowing applications to pre-register a *PeerGroup* to target with low-latency bulk transfers.

Transfers execute between two devices: it is up to the user to coordinate operations across multiple devices in a system.

UVM Watcher In order for the host to be able to initiate transfers upon GPU progress, `alloc_uvm_watcher` registers a callback invoked upon changes to a word in memory. It allocates a unified virtual memory (UVM) location that can be updated by the devices, including kernels within a CUDA graph, which is continuously polled by a CPU thread using GDRCopy. Since not all changes are guaranteed to be observed immediately, the callback is invoked the old and the new values, allowing it to respond to GPU-side progress.

Completion Notification Notifications are delivered for both send confirmation and receive completion, either through callbacks or atomic flags. The IMM_COUNTER is a dedicated component that keeps track of per-immediate counters incremented on events retrieved from the completion queue of the underlying devices. Events are generated on the sender after a transfer is completed and on the receiver once a payload with an immediate attached to it has been fully delivered, guaranteeing atomicity. The counters are allocated in the same NUMA node as the domain worker.

The counters can either be transparently synchronized with the GPU via GDRCopy, observed directly through polling or handed off to a callback on a separate dedicated thread within the engine, registered using `expect_imm_count`. All synchronization is implemented using such counters, as

otherwise there are no other ordering guarantees.

Correctness of IMM_COUNTER under unordered transport relies on PCIe ordering guarantees: the RDMA specification requires that the data payload of a WRITE_IMM is issued before the immediate value, and the PCIe switch guarantees ordering of writes targeting the same device. Although the immediate value targets the CPU while the data targets the GPU, the host-proxy architecture avoids data races: after the CPU observes the target IMM_COUNTER, any subsequent CPU-to-GPU transaction (e.g., launching a kernel or updating a flag via GDRCopy) is ordered by the PCIe switch after the preceding NIC-to-GPU data writes, ensuring the payload is visible to the GPU.

3.4 Implementation

Our *TransferEngine*, implemented in Rust, carefully optimizes allocations, threading and synchronization to minimize latency in order to achieve high throughput. The engine spawns one worker thread per DOMAIN_GROUP, each pinned to a CPU core on the NUMA node to which the devices are attached to minimize both scheduling and memory access latency. Data structures specific to a domain are allocated after pinning to ensure that memory is reserved in the correct NUMA node. One worker thread is responsible for handling up to 4 DOMAINS, each managing a single NIC, whereas another dedicated thread is responsible for polling the GPU to update UVM watchers. Cross-thread communication is done through lock-free queues.

The API forwards requests to the DOMAIN_GROUP serving the appropriate device, with the first one also serving the host. In a tight loop, the domain worker polls for new work, prioritizing the submission of new requests. Depending on the hardware and configuration, requests are sharded and load-balanced across the available DOMAINS. The first WRITE of a composite request is immediately posted to the NIC's send queue in the DOMAIN. Once new requests are exhausted, the worker proceeds to progress on pending, posting writes to fill up the hardware pipeline. Subsequently, completion queues are polled to query for finished transfers and immediate counter increments. Events are aggregated to deliver per-transfer notifications, handing the transfer over to a dedicated callback thread shared by all groups.

Sharding inside a DOMAIN_GROUP is flexible. Transfers can target specific NICs by index. A single WRITE can be split. Paged transfers, scatter and barrier operations, which all translate to multiple WRITES, can shard across all NICs.

3.5 Hardware-Specific Optimizations

The DOMAINS within the *TransferEngine* are specialized and optimized for the hardware under their control:

AWS EFA We implement EFA support using *libfabric*,

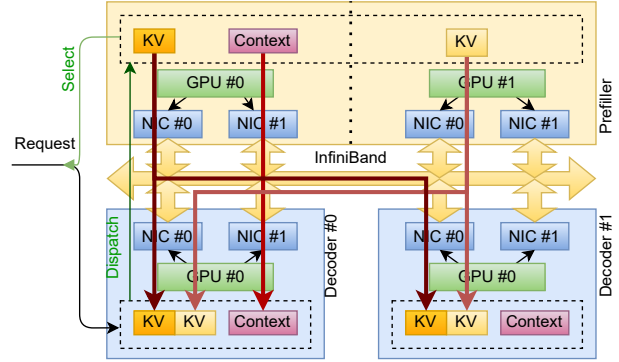


Figure 3. KV transfer between prefillers and decoders

managing a fabric domain per NIC within the DOMAIN_GROUP. Since EFA diverges from the RDMA spec which does not require a valid target descriptor for immediate-only zero-sized writes, we enforce a valid descriptors for all transfers. For bulk transfers and peer groups, we employ work request (WR) templating, pre-populating and retaining the common fields of *libfabric* descriptors before posting.

NVIDIA ConnectX-7 We implement ConnectX support through *libverbs*. For each peer, we use an UD queue pair to exchange RC handshakes. We create 2 RC queue pairs per peer: one for two-sided SEND/RECV operations and another for one-sided WRITE and WRITE_IMM operations. This separation is necessary because both RECV and WRITE_IMM completions consume work requests in posting order. This allows us to provide high-level RECV semantics while supporting WRITE_IMM without interference. In addition to WR templating, we employ WR chaining by linking up to 4 work requests through the `next` pointer of `ibv_send_wr`, reducing the number of doorbell rings to the NIC. Additionally, we enable `IBV_ACCESS_RELAXED_ORDERING` to permit out-of-order PCIe transactions between the NIC and GPU memory, reducing latency.

4 KVCACHE TRANSFER

In this section, we outline a production-tested implementation of disaggregated inference relying on the *TransferEngine*. Pseudocode is provided in Appendix A. In disaggregated mode, a prefiler node runs prefill on the input tokens, transferring the resulting KV pages and any additional context, such as last token hidden states and logits for speculative decoding, to the decoder node which proceeds to decode tokens one-by-one.

Figure 3 illustrates our disaggregated setup. Once a request is received, a global scheduler selects a prefiler node and a decoder node to process it and forwards the request to the decoder. The decoder pre-allocates KV pages and storage for any context before dispatching the request to the designated prefiler using `submit_send`, indicating the KV page indices where contents should be transferred to.

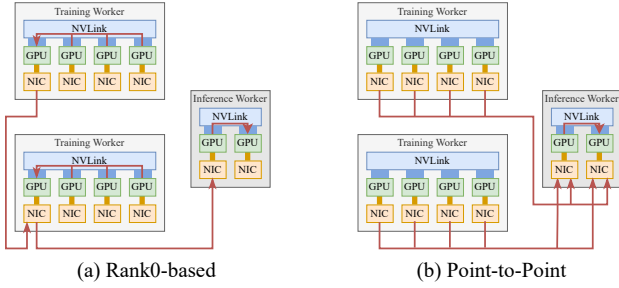


Figure 4. Weight transfer data path for different approaches.

During chunked prefill, we increment the UVM watcher value after the attention output projection of each layer, which is CUDA Graph compatible. Once *TransferEngine* detects the change in the UVM watcher value, the layer’s transfer is initiated, copying over the pages from the current chunk via `submit_paged_writes`. When the last chunk is complete and the context has been populated, it is copied over via `submit_single_write`. Prefillers await for commands using `submit_recv`s.

KV transfers must account for differences in the sharding or replication of KvCaches between prefillers and decoders. MLA (Liu et al., 2024) replicates the compressed KvCache entries if tensor parallelism is used: under such a scheme, prefiller ranks are randomly matched with decoder ranks to balance the transfers of replicas. Under GQA (Ainslie et al., 2023), we rely on page-wise offsets and strides to select slices from the source KvCache to copy into corresponding offsets in the destination KvCache. To minimize the number of writes and ensure that individual writes are sufficiently large, the KvCaches are laid out with heads preceding the pages, ensuring continuity within consecutive heads.

The prefiller does not issue an explicit completion message: the decoder knows in advance the number of transfers it expects and uses `expect_imm_count` to be notified by the *TransferEngine* of transfer completion and start decoding.

The complexity of a production-ready implementation of disaggregated decoding lies in the handling of errors and cancellation. Cancellation triggered by a decoder must be explicitly confirmed by the prefiller, as the KV pages cannot be reused as long as there is a possibility of a remote write clobbering them. We rely on heartbeat messages between prefillers and decoders to detect transport layer failures. If a prefiller node is unresponsive, requests are cancelled on the decoder after a timeout, as transfers can no longer reach it. A per-request cancellation token can stop all future transfers whilst also waiting after all pending operations before sending the cancellation confirmation.

5 RL ROLLOUT WEIGHT TRANSFER

In asynchronous reinforcement learning fine-tuning, training and inference run on separate GPUs. After each training

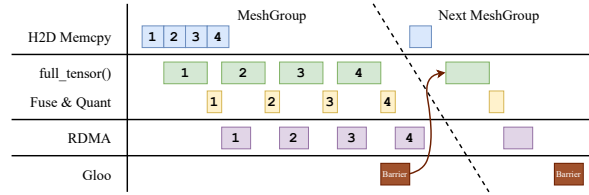


Figure 5. Pipelined weight transfer execution.

step, new weights must be pushed to inference nodes, which can take tens to hundreds of seconds on trillion-parameter models using existing frameworks. Our solution achieves 1.3-second cross-machine parameter updates for models at the scale of Kimi-K2 (1T parameters), DeepSeek V3 (671B) and Qwen3 (235B) (Kimi Team et al., 2025; DeepSeek-AI et al., 2025; Yang et al., 2025), transferring weights from 256 training GPUs (bf16) to 128 inference GPUs (fp8).

5.1 Point-to-Point Weight Transfer

Existing frameworks tend to form a global collective communication world for all training and inference GPUs. Weights are gathered to training sub-group *Rank0*, then broadcast to *Rank0* of each inference sub-group, bottlenecked by the NIC of training *Rank0*. In contrast, in our P2P approach each training GPU send weights directly to inference GPUs via one-sided RDMA WRITE, utilizing the full cluster bandwidth across all NICs. Figure 4 illustrates the difference between the two approaches.

At initialization, the controller script performs three steps: First, it gathers parameter metadata from all training and inference GPUs, including weight name, shape, dtype, and DTensor sharding. Next, it computes a static weight transfer schedule, mapping which training GPU sends which parameter to which inference GPU, and in what order. Finally, it broadcasts the schedule to all training GPUs. Appendix B provides pseudocode for this workflow.

At each training step, the controller signals training GPUs to begin sending weights. The inference nodes remain unaware of the transfer, as it uses one-sided operations.

5.2 Pipelined Weight Transfer Execution

Our training job shards model weights using FSDP (Zhao et al., 2023). Different parameter types (e.g., MoE vs non-MoE) require different FSDP sharding strategies. Each sharding strategy partitions the global DeviceMesh into disjoint sub-meshes. We call each sub-mesh a *MeshGroup*. Parameters within a *MeshGroup* are transferred in parallel, while *MeshGroups* are processed sequentially.

We treat the transfer of each parameter tensor as a *task*. To utilize different hardware resources simultaneously, we split each task into four pipeline stages that overlap in time, as illustrated in Figure 5: (1) Host-to-device memcopy if FSDP

offloads weight to CPU. (2) Parameter preparation: Reconstruct full weight with `full_tensor()`, apply projection fusion, quantize if needed. (3) RDMA transfer: Zero-copy WRITE to remote inference GPU memory. (4) Global barrier: After all `full_tensor()` calls are done, synchronize across mesh groups using GLOO via Ethernet.

`full_tensor()` and other GPU operations introduce extra GPU memory usage. To avoid out-of-memory errors, we only start a new task if the current in-flight tasks occupy less temporary GPU memory than a configurable watermark.

6 MOE DISPATCH/COMBINE

We present a set of low-latency kernels for MoE dispatch and combine built around the *TransferEngine*, relying on a host proxy thread to coordinate the GPUs and the NICs. Within a node, we also utilize NVLink to reduce the load on the network. Despite the added latency of a proxy thread, we achieve state-of-the-art decode performance while maintaining competitive performance for prefill without any tweaks.

These kernels demonstrate the feasibility of proxy-based MoE dispatch with support for a wider range of network cards, such as EFA. Consequently, we focus on decode performance (up to 128 tokens per rank) as it is latency-bound, suffering more significantly from the added PCIe, driver and firmware overheads across the devices involved.

6.1 Architecture

Routing is implemented using split kernels for both decode and combine, with a sender half preparing the data into send buffers to be written to peers and a receiver half shuffling tokens from receiver buffers into tensors used by other kernels. The individual kernels fully utilize all SMs and the memory bandwidth of the GPU to reduce latency, however their runtime is short enough to interleave other work between them, enabling overlapping and micro-batching. The host proxy uses GDRCopy to poll the GPU for progress, invoking the *TransferEngine* when source buffers are ready.

Our design, illustrated in Figure 6, minimizes the proxy overhead by reducing the number of writes issued. To reduce the GPU memory required for send and receive buffers, all peers first exchange routing information, per-expert token counts, to determine a unique range in a contiguous receive buffer to write to. Since these payloads are small, their latency is hidden by speculatively dispatching a small number of tokens into private per-source buffers. Combine issues a single scatter as it re-uses the routing information. Routing information is always handled by the *TransferEngine*, but payloads can be copied via NVLink within the same node. Consequently, each rank issues up to 2 WRITES for dispatch and 1 WRITE for combine for each inter-node peer.

Receiver buffers must be sized to account for all tokens being sent to the current rank. Assuming there are N ranks hosting E experts, each dispatching T tokens to R experts, the upper bound is $N \cdot T \cdot \max(R, \frac{E}{N})$. Senders pack writes into such a contiguous buffer instead of relying on larger per-rank receiver buffers. To minimize overhead, the larger dispatch receive buffer can be re-used by combine send.

6.2 Dispatch

The dispatch kernel receives the tokens and the R indices of the experts to which they must each be routed, returning a tensor which packs the tokens from all the ranks assigned to the local experts. The kernel first counts the number of tokens sent to each expert in shared memory and transfers the counts to the host via unified memory. It then signals the proxy, which uses the *TransferEngine* to initiate the scatter of the routes to all peer ranks. The input tokens are then copied into the send buffers, creating a contiguous source to be scattered to each peer, as shown in Figure 7.

The proxy is notified to scatter tokens up to a fixed limit into private buffers on each receiver peer. For decode-sized batches, the latency from the launch of the dispatch kernel to the first transfer is around $15 \mu\text{s}$ assuming EP=64. At this point, the transfers of routes and tokens saturate the NIC bandwidth. Once the routes are received and the position of tokens from each source rank can be determined on each destination rank, the remainder of the tokens are scattered to the peers, placing them contiguously into a shared receiver buffer. The host-side work to process routes and dispatch the second round of transfers takes tens of microseconds. The number of tokens in the initial transfer is chosen to hide this overhead. Although this latency is not on the critical path, reducing it can further reduce the size of the private buffers. Once all transfers are acknowledged as having completed and all incoming writes are accounted for, a barrier synchronizes the proxies via the *TransferEngine*.

Following the dispatch of transfers to inter-node peers over RDMA, the send kernel proceeds to issue writes over NVLink to transfer tokens within the same node, while RDMA transfers are pending in the background. NVLink peers synchronize themselves through their own set of barriers: before writing to a peer, each rank must ensure that the data has been read and can be overwritten. This is done through flags written and read with relaxed semantics. After the payloads are written, ranks synchronize through release-acquire flags with each other.

Write ordering in send kernels is latency-critical due to the lack of granularity in memory barriers. NVLink is exposed via virtual memory, transparently translating reads and writes to peer devices mapped into the current address space into transactions on the interconnect. Loads are universally expensive, as they block the execution pipeline until

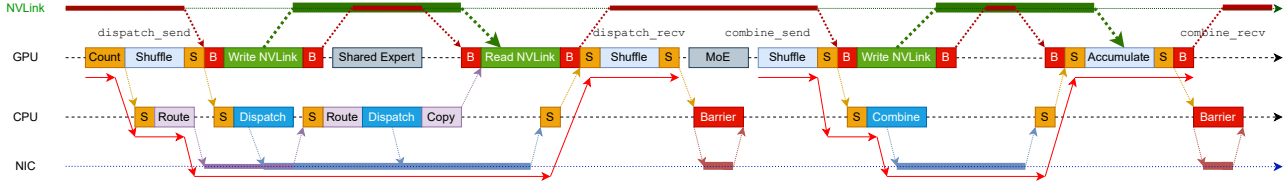


Figure 6. Dispatch and Combine GPU-CPU-NIC coordination

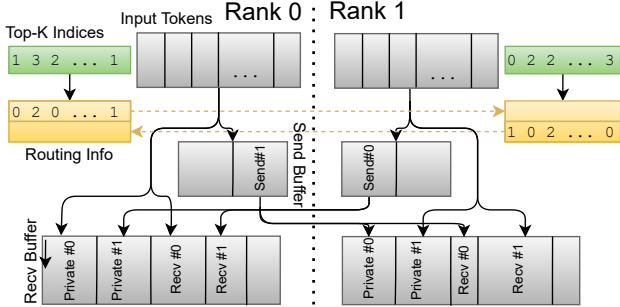


Figure 7. Dispatch into private and contiguous buffers

they are satisfied. In contrast, stores are fire-and-forget, until a memory barrier is encountered, which blocks until all prior stores within their scope complete. Since both the host system and NVLink peers are within the same scope, a barrier ensuring ordering with the host might be slowed down by previously issued writes over NVLink. This is avoided by first signalling the host, then issuing NVLink writes after a grid barrier. This strategy increases the total execution time of send kernels, but it reduces latency on the critical path to the first RDMA transfer.

With NVLink, it is usually preferable to push data from a source device to a target, saving a trip time. Additionally, after the stores are acknowledged on the current device, useful work can be executed while the transfers are in-flight to the remote. With dispatch, we only push the tokens to the private receive buffers, since at this stage the centralized routing information is not available to determine exactly where the rest of the tokens should be placed on the peer. The receiver half of the kernel kicks off by synchronizing on the barrier and reading the remaining tokens. These loads are likely to complete before the RDMA operations.

After dispatch send, transfers run in the background. Once the receiver kernel is called, it waits for the *TransferEngine* to report the completion of all transfers via *IMMCOUNTER* and *GDRCopy*. Relying on indices computed based on the routing information, tokens are re-ordered with optional padding between experts following a layout suitable for Grouped GEMM kernels. Since the receiver kernels must process around $T \cdot R$ tokens while on the critical path, work is split across all available SMs and pipelining is maximised to fully utilize the available HBM bandwidth.

6.3 Combine

Since routing information is centralized during the dispatch stage, combine transfers all payloads in a single scatter. The command is prepared during the idle time between send and combine, during which the GPU would typically execute a grouped GEMM. The sender, similarly to dispatches, prepares send buffers and pushes tokens via NVLink to intra-node peers. The host proxy is signalled to send the *SCATTER* requests to the *TransferEngine*, after which the kernel finishes execution. The receiver caches all relevant offsets derived from routing information in shared memory before waiting for all tokens to be received. The weighted average of the tokens is then computed locally on each rank.

The combine stage re-uses the same buffers as the dispatch stage, thus it requires both an NVLink and an RDMA barrier ensuring the completion of all prior operations before overwriting the send buffers. At this point, the host proxy also waits for the *TransferEngine* to confirm that all writes have been sent out. Particularly for EFA, which also waits for receipt confirmation, it is important to maximise the interval between posting a write and checking its status.

6.4 Comparison with DeepEP

DeepEP offers state-of-the-art latency, however they are tied to ConnectX due to their reliance on IBGDA and `m1x5` driver. Our kernels are more portable, relying on a host proxy, supporting both EFA and ConnectX. Despite the added overhead, our latency exceeds DeepEP.

DeepEP kernels rely on the strong ordering guarantees of RC QP. The tokens are balanced across the available SMs which transfer them over a QP one-by-one. This ensures a lower latency to the first transfer, however it also involves more work on a per-token basis and results in more packets being sent over the network. Token counts and completion are signalled via *ATOMICS*. In contrast, our kernels spend more time before the first transfer is initiated due to the additional GPU-CPU-NIC communication overheads over PCIe. However, bulk transfers achieve better network utilization.

For prefill, we scale our single-transfer strategy without tweaks. In contrast, DeepEP achieves better latencies by pre-accumulating tokens via NVLink on the sender node, reducing the amount of data transferred. Additionally, the

DeepEP kernels use less buffer memory as subsets of tokens are transferred in batches. While this approach is faster, it also has implications on accuracy and determinism, as accumulation it not done entirely on fp32 in a fixed order.

7 EVALUATION

We evaluate on two cluster configurations: $8 \times H200$ nodes with 2×200 Gbps EFA per GPU, and $8 \times H100$ nodes with 400 Gbps ConnectX-7 per GPU. End-to-end evaluations run on a custom inference engine built on PyTorch.

7.1 Point-to-Point Communication

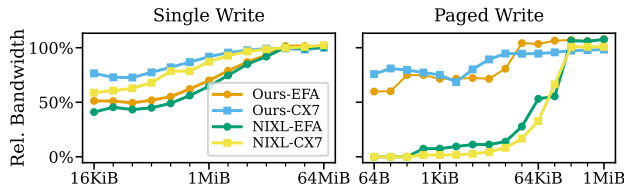


Figure 8. Point-to-Point communication performance

	EFA		CX-7		
Single	64 KiB	16 Gbps	44 Gbps		
	256 KiB	54 Gbps	116 Gbps		
	1 MiB	145 Gbps	245 Gbps		
	32 MiB	336 Gbps	378 Gbps		
Paged	1 KiB	17 Gbps	2.11M op/s	91 Gbps	11.10M op/s
	8 KiB	138 Gbps	2.10M op/s	320 Gbps	4.89M op/s
	16 KiB	274 Gbps	2.08M op/s	367 Gbps	2.80M op/s
	64 KiB	364 Gbps	0.69M op/s	370 Gbps	0.71M op/s

Table 2. EFA and ConnectX-7 performance comparison

The performance of KvCache transfers and RL rollouts is determined by the throughput of single and paged writes. We compare higher-level libraries (*TransferEngine* and *NIXL* v0.6.1) against hardware benchmarks for the underlying NICs, measuring the fraction of bandwidth for a range of message sizes. On ConnectX we compare against `ib_write_bw` from *rdma-core*. On EFA, we use `fi_rma_bw` from *libfabric* to measure peak single-NIC bandwidth, which we double to match the engine running on two NICs.

Figure 8 shows the fraction of the peak bandwidth achieved by both libraries. To saturate with single WRITE, messages of at least 16MiB are required, while 32KiB and 64KiB are sufficient to saturate with paged WRITE on both *TransferEngine* and *NIXL*, respectively. Performance between our solution and *NIXL* is relatively close, with the *TransferEngine* being slightly faster. EFA requires larger messages to saturate, explaining the gap observed on MoE routing.

Table 2 details absolute performance numbers. For 256 KiB single WRITE (typical for our MoE routing), our *TransferEngine* achieves 54 Gbps on EFA and 116 Gbps on

ConnectX-7. At 64 KiB paged WRITE (typical size for a KvCache page), both EFA and ConnectX-7 are able to saturate the available bandwidth. The size of RL weight transfer messages is well beyond the saturation point.

7.2 KvCache Transfer

SeqLen	TTFT (ms)		Per-layer (ms)		Steps	Pages
	Non-	Disagg	Compute	Transfer		
4K	214	260	2.267	0.661	1	256
8K	433	501	4.578	0.952	1	512
16K	929	1042	9.860	1.610	1	1024
32K	2179	2317	13.295	1.606	2	1024
64K	5681	5852	20.344	1.611	4	1024
128K	16735	17056	34.895	1.609	8	1024

Table 3. KvCache transfer impact on TTFT (Qwen3-235B, H200 TP4, 2×200 Gbps EFA)

Table 3 shows the end-to-end impact of disaggregated KvCache transfer on TTFT for Qwen3-235B on H200 with TP4 and 2×200 Gbps EFA per GPU. We use a KvCache page size of 32 kB (128 tokens) with chunk-prefill length up to 16384 tokens, CUDA Graph enabled, and UvmWatcher to detect layer completion. Although 1024 pages of 32 kB cannot saturate RDMA bandwidth, layer-by-layer KvCache transfer is still hidden by computation. The observed TTFT slowdown relative to non-disaggregated execution is mainly from our inference engine performing one extra decode pass for the final input token, rather than from KvCache transfer.

Callback	avg	min	p50	p90	p99	p99.9	max
Rust	6.3 ± 1.3	2.5	6.2	7.0	12.6	19.4	64.8
Python	9.8 ± 9.0	6.1	9.3	11.1	20.4	41.7	3325.0

Table 4. UvmWatcher callback latency under CUDA Graph (μ s)

Table 4 reports the tail latency of UvmWatcher callbacks under CUDA Graph. When the callback is in Rust, latency is tightly bounded, only slightly above the 2μ s to 5μ s PCIe latency. With Python, overhead is still acceptable.

7.3 RL Weight Transfer

Operation	Time	Avg. per-call	Count
Total	1233 ms	—	—
Memcpy H2D	184 ms	378 μ s	487
full_tensor()	518 ms	532 μ s	974
Fuse projections	18 ms	37 μ s	487
Quantize	88 ms	137 μ s	647
RDMA submit	26 ms	23 μ s	1144
Waiting for other ranks	357 ms	—	—
Remaining*	42 ms	—	—

* Includes extra RDMA time not hidden by other operations.

Table 5. RL weight transfer latency breakdown for one rank

Table 5 shows a per-rank latency breakdown for transferring Kimi-K2-1T weights from 256 training GPUs (BF16,

FSDP/PP/EP=16/2/8) to 128 inference GPUs (FP8, EP=32), profiled with PyTorch profiler. The total transfer completes in 1.2 s, an order of magnitude faster than the 10 s to 100 s reported by prior systems for comparable model sizes (Moonshot AI, 2025; Li, 2025; He, 2025; He et al., 2025).

The breakdown confirms effectiveness of the pipelining shown in Figure 5. The critical path is dominated by `full_tensor()` for FSDP parameter unsharding (518 ms) and synchronization across ranks (357 ms). RDMA transfers run concurrently with parameter preparation; only 42 ms of transfer time falls outside the pipeline overlap. The CPU overhead of posting 1144 RDMA work requests is 26 ms. Our training logs for DeepSeek-V3-671B and Qwen3-235B show similar transfer times of 1.2 s to 2 s.

7.4 MoE Dispatch/Combine

We evaluate the performance of the MoE kernels for both decode and prefill across 8, 16, 32 and 64 GPUs, comparing them to DeepEP, which is the most performant open-source implementation, as well as the portable and open-source *pplx-kernels* (Licker et al., 2025) which are built around NVSHMEM v3.4.5, running on both EFA and ConnectX-7. While there is overlap between our work and UCCL-EP (Mao et al., 2025), we do not include a detailed comparison as their published latencies are substantially higher. We show that on ConnectX-7 adapters our performance is the new state-of-the-art, despite the use of the host proxy.

7.4.1 End-to-End Decode Speed

Cluster	Kernel	batch=2	batch=8	batch=32
H200 EFA	Ours	66.752	56.459	32.003
	<i>pplx-kernels</i>	20.972	11.607	4.903
H100 CX-7	Ours	78.420	67.666	36.066
	DeepEP	73.758	65.785	36.253

Table 6. End-to-end MoE decode speed (tokens/s, DeepSeek-V3, MTP, EP=DP=64)

Table 6 reports end-to-end decode speed of DeepSeek-V3 with MTP (draft length 1, acceptance rate 80%) at EP=DP=64. On EFA, our kernels achieve 3–6× higher throughput than *pplx-kernels*, making real-time inference practical on EFA for the first time. On ConnectX-7, our kernels match or slightly exceed DeepEP across all batch sizes, despite using a host proxy rather than GPU-initiated RDMA. The two implementations share the same inference engine and differ only in the MoE dispatch/combine kernel.

7.4.2 Computation–Communication Overlap

Dual-batch overlap pipelines computation of one batch with communication of another, and is effective only when the per-GPU batch size is sufficiently large. (Perplexity AI,

Batch	Ours		<i>pplx-kernels</i>	
	no overlap	dual-batch	no overlap	dual-batch
128	11.813	13.916	1.548	1.454
96	14.349	16.487	2.006	1.807
64	21.260	21.436	2.824	2.432
48	24.223	24.197	3.584	3.272
32	32.003	30.237	4.903	4.827

Table 7. End-to-end MoE decode speed (tokens/s) with and without dual-batch overlap (DeepSeek-V3, MTP, EP=DP=64, EFA)

2025; vLLM, 2025; SGLang, 2025) Table 7 shows that even in throughput-oriented regimes, MoE dispatch/combine latency still matters: overlap provides only modest gains for our kernels and consistently degrades performance for *pplx-kernels* due to their high communication latency. For latency-sensitive workloads with small batches, computation and communication are sequential due to data dependencies, making low communication latency essential.

7.4.3 Kernel Microbenchmarks

Microbenchmark Setup. To compare with DeepEP, our kernel-level benchmarks consider the settings of DeepSeek-V3/R1 model. We dispatch $7168 \times \text{fp8}$ tokens with $56 \times \text{fp32}$ scaling factors and combine bf16 tensors of the same dimension. Decode is evaluated on batches of 128, prefill on chunks of 4096 tokens. Each token is dispatched to 8 random experts. We run 10,000 warmup iterations, followed by 10,000 benchmarked runs, aggregating timing across all ranks. We simulate overlapped work and clear caches by inserting large GEMMs.

Decode Latency. Figure 9 shows the latencies of our MoE dispatch and combine kernels on decode-sized batches, comparing them to the specialized DeepEP and the portable *pplx-kernels*. Our proxy-based implementation not only makes EFA viable, it is also faster than the IBGDA-based kernels on ConnectX-7 and an order of magnitude faster than the NVSHMEM kernels using IBRC through the generic host proxy.

In the intra-node setup with 8 ranks, our kernels are slower by about $2 \mu\text{s}$ than DeepEP, largely due to the use of NICs to exchange routing information. Whilst this data point is not critical for our primary inter-node use case, it does highlight that the NVLink transfers whose latencies are otherwise hidden by RDMA are highly efficient. *pplx-kernels* rely on fine-grained per-token NVLink synchronization under this configuration. The discrepancy is due to bulk transfers and per-block/per-grid synchronization over NVLink.

Inter-node on 16 and 32 ranks our kernels outperform DeepEP on both dispatch and combine, largely due to the bulk transfers and efficient pipelining in the combine phase. The ordering of RDMA and NVLink writes also helps reduce the latency to the first RDMA transfer. When scaling

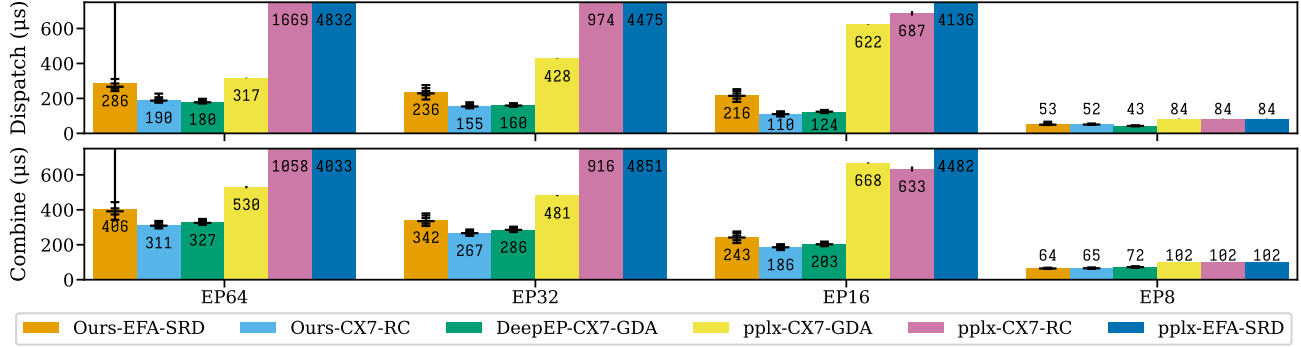


Figure 9. MoE Decode Latency. Bar height is mean. Error bars show p01, p25, p50, p75, p95, p99. Error bars for *pplx* indicate stddev.

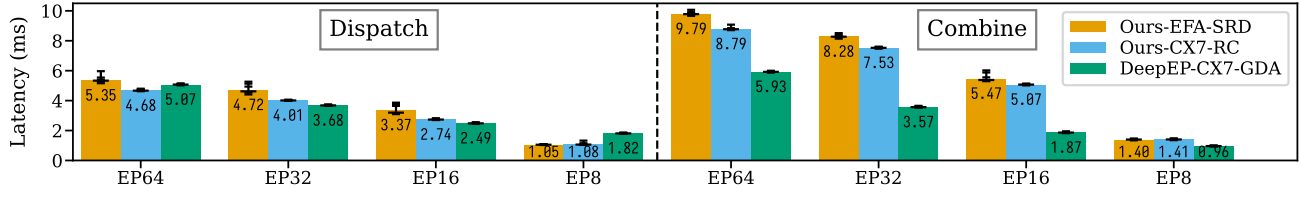


Figure 10. MoE Prefill Latency. Bar height is mean. Error bars show p01, p25, p50, p75, p95, p99.

to 64 ranks, combine still outperforms DeepEP, but the CPU overhead of the proxy thread becomes noticeable and dispatch is slower due to the roughly microsecond overhead of enqueueing a transfer for each of the 56 inter-node peers.

Since the bandwidth is not saturated by decode, EFA latencies are trailing behind by only 30%, despite 256KiB writes achieving less than half of the ConnectX-7 throughput.

Prefill Latency. Figure 10 shows the latency of MoE Prefill. We exclude *pplx-kernels* from the comparison as they are not effective at 4096 tokens. Due to the lack of chunking in transfers, the memory overhead of our decode-optimized kernels limits the set of models for which a deployment is viable.

On the dispatch side, DeepEP performs better with fewer ranks as they use RDMA to transfer only one replica of the token, moving copies of it to other ranks via NVLink. At EP64, where the chances of multiple replicas landing on the same node are smaller, the effect of this optimization tapers off. On combine, DeepEP’s sender-side partial sum greatly reduces RDMA bytes, hence shows much lower latency, despite the reduced accumulation precision to bf16.

7.4.4 Ablation: Private Buffer Size

The private buffers were designed to hide the latency of routing information exchange. We compare the median latency of total decode dispatch times while varying the number of tokens with the peak latency achieved with a buffer size that can accommodate all tokens in one burst.

Figure 11 indicates the performance dropoff as the private

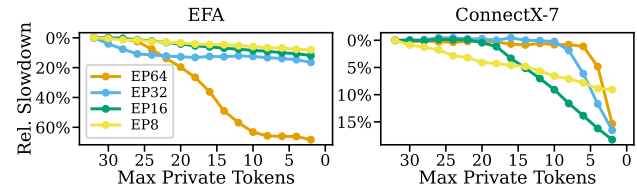


Figure 11. Impact of private buffer size on p50 decode latency

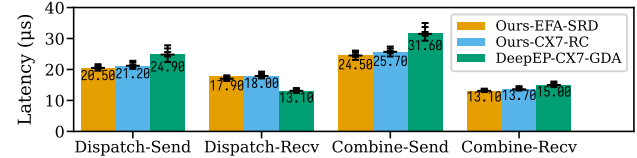


Figure 12. Separate Send and Receive Latency for EP=64

buffer size decreases. The performance degradation in the absence of tokens justifies the use of the latency-reduction strategy. In the intra-node case, where tokens are transferred faster, at least around 32 tokens are necessary to hide the latency of route exchange across both NICs. In the inter-node case, ConnectX-7 NICs allow as few as 24 tokens to be used, while EFA NICs present a performance dropoff under 32 tokens already, since route exchange is slower.

7.4.5 Ablation: Send and Receive Latency

Our kernels, similarly to DeepEP, are split into senders and receivers, with both NVLink and RDMA transfers executing in the background between them. Figure 12 shows these latencies, which were measured by inserting a long artificial delay simulating shared experts or overlapped work before the receive kernels, allowing all transfers to settle.

Dispatch and combine send outperform DeepEP as ours only

Event	Thread	p50	p90	p99	p99.9
submit_scatter()	App	—	—	—	—
→ Enqueue done	App	0.120	0.156	2.019	3.484
→ Worker enqueue done	Worker	0.855	1.036	1.450	5.050
→ Before posting first WRITE	Worker	0.441	0.535	0.736	4.889
→ After posting last WRITE (EFA)	Worker	27.886	30.240	39.176	43.323
→ After posting last WRITE (CX-7)	Worker	8.502	9.151	12.310	14.474

Table 8. CPU overhead breakdown for MoE all-to-all with EP64 (μ s)

copy memory. Due to faster accumulation, combine receive is also faster. Dispatch receive is an outlier, since it pulls data using NVLink loads. Overall, the total execution time of these kernels is under 15% of the transfer times. More in-depth profiling reveals the proxy commences RDMA work midway through the execution of the send kernels, with shuffling adding only about 15 μ s of idle time.

7.4.6 Ablation: Host-Proxy Overhead Breakdown

NIC	EP	p50	p90	p99	p99.9
EFA	EP8	3.081	3.348	4.769	13.175
	EP16	6.536	7.141	8.429	17.067
	EP32	13.374	14.412	22.633	26.803
	EP64	27.886	30.240	39.176	43.323
CX-7	EP8	0.842	0.893	1.162	3.281
	EP16	1.926	2.049	2.853	5.516
	EP32	4.140	4.392	5.830	8.709
	EP64	8.502	9.151	12.310	14.474

Table 9. Post time for all WRITES of scatter (μ s)

Table 8 instruments key events during MoE kernels with EP64, reporting the elapsed time since the previous event. *TransferEngine* incurs minimal CPU overhead from the application call to the first RDMA WRITE: under 1.5 μ s at p50. The dominant cost is posting the WRITES themselves, which includes overhead inside `libfabric` for EFA.

Table 9 shows how posting time scales with the number of scatter targets. Posting time increases roughly linearly with expert parallelism, but remains acceptable: at EP64 on ConnectX-7, the total posting time is under 10 μ s at p50, and on EFA under 28 μ s. As shown in Figure 9, this overhead does not prevent our kernels from matching or exceeding DeepEP performance.

8 DISCUSSION

GPU-Initiated Communication GPU-initiated RDMA (GDA) bypasses the host CPU to reduce latency. GDA is not yet available on most cloud instances (AWS p5/p5e, eRDMA) and remains preliminary on p5en; our host-proxy design serves this current-generation hardware while preserving portability. For MoE, next-generation GPUs with wide NVLink domain (e.g., GB200 NVL72) shift communication off RDMA entirely. For KvCache and RL weight

transfers, RDMA latency is already hidden by computation, so our CPU-based approach frees the GPU without sacrificing end-to-end performance.

Supporting Additional NICs The *TransferEngine* currently supports ConnectX and EFA. Among Linux rdma-core providers, only EFA diverges from the standard RC transport. For RC-compatible NICs (e.g., eRDMA, Broadcom, AMD), the internal implementation would resemble the ConnectX path. Porting to additional NICs requires per-hardware tuning, not a redesign of the library; application code built on the *TransferEngine* API remains unchanged.

9 CONCLUSION

Existing RDMA solutions for LLM systems suffer from vendor lock-in, with no viable implementations on custom cloud hardware such as AWS EFA. `fabric-lib` addresses this by identifying common functionality across heterogeneous RDMA hardware. By layering a reliable abstraction without ordering guarantees over the underlying protocols, we transparently extended support to multiple RDMA NICs, with a particular focus on EFA and ConnectX.

We demonstrated this approach through three production systems: KvCache transfer for disaggregated inference, RL weight updates achieving 1.3 seconds for trillion-parameter models, and MoE dispatch/combine with state-of-the-art latency on ConnectX-7 and the first viable implementation compatible with AWS EFA. `fabric-lib` enables portable point-to-point communication for modern LLM architectures, avoiding vendor lock-in while complementing collective libraries for cloud-native deployments.

ACKNOWLEDGEMENTS

We thank NVIDIA for generously providing access to the ConnectX-7 hardware for our evaluations, alongside valuable insights towards maximizing performance on H200 GPUs. We thank AWS for their insights and advice towards improving performance on EFA.

REFERENCES

- Agostini, E., Rossetti, D., and Potluri, S. GPUDirect async: Exploring GPU synchronous communication techniques for InfiniBand clusters. *J. Parallel Distributed Comput.*, 114:28–45, 2018. doi: 10.1016/J.JPDC.2017.12.007. URL <https://doi.org/10.1016/j.jpdc.2017.12.007>.
- Ainslie, J., Lee-Thorp, J., De Jong, M., Zemlyanskiy, Y., Lebrón, F., and Sanghai, S. Gqa: Training generalized multi-query transformer models from multi-head checkpoints. *arXiv preprint arXiv:2305.13245*, 2023.
- Alibaba Cloud. Elastic compute service: eRDMA, 2025. URL <https://www.alibabacloud.com/help/en/ecs/user-guide/elastic-rdma-erdma/>.
- Chang, L.-W., Bao, W., Hou, Q., Jiang, C., Zheng, N., Zhong, Y., Zhang, X., Song, Z., Jiang, Z., Lin, H., Jin, X., and Liu, X. Flux: Fast software-based communication overlap on gpus through kernel fusion, 2024.
- DeepSeek AI. Fire-flyer file system (3fs). <https://github.com/deepseek-ai/3FS>, 2025. High-performance distributed file system for AI training and inference workloads.
- DeepSeek-AI, Liu, A., Feng, B., Xue, B., Wang, B., Wu, B., Lu, C., Zhao, C., Deng, C., Zhang, C., Ruan, C., Dai, D., Guo, D., Yang, D., Chen, D., Ji, D., Li, E., Lin, F., Dai, F., Luo, F., Hao, G., Chen, G., Li, G., Zhang, H., Bao, H., Xu, H., Wang, H., Zhang, H., Ding, H., Xin, H., Gao, H., Li, H., Qu, H., Cai, J. L., Liang, J., Guo, J., Ni, J., Li, J., Wang, J., Chen, J., Chen, J., Yuan, J., Qiu, J., Li, J., Song, J., Dong, K., Hu, K., Gao, K., Guan, K., Huang, K., Yu, K., Wang, L., Zhang, L., Xu, L., Xia, L., Zhao, L., Wang, L., Zhang, L., Li, M., Wang, M., Zhang, M., Zhang, M., Tang, M., Li, M., Tian, N., Huang, P., Wang, P., Zhang, P., Wang, Q., Zhu, Q., Chen, Q., Du, Q., Chen, R. J., Jin, R. L., Ge, R., Zhang, R., Pan, R., Wang, R., Xu, R., Zhang, R., Chen, R., Li, S. S., Lu, S., Zhou, S., Chen, S., Wu, S., Ye, S., Ye, S., Ma, S., Wang, S., Zhou, S., Yu, S., Zhou, S., Pan, S., Wang, T., Yun, T., Pei, T., Sun, T., Xiao, W. L., Zeng, W., Zhao, W., An, W., Liu, W., Liang, W., Gao, W., Yu, W., Zhang, W., Li, X. Q., Jin, X., Wang, X., Bi, X., Liu, X., Wang, X., Shen, X., Chen, X., Zhang, X., Chen, X., Nie, X., Sun, X., Wang, X., Cheng, X., Liu, X., Xie, X., Liu, X., Yu, X., Song, X., Shan, X., Zhou, X., Yang, X., Li, X., Su, X., Lin, X., Li, Y. K., Wang, Y. Q., Wei, Y. X., Zhu, Y. X., Zhang, Y., Xu, Y., Xu, Y., Huang, Y., Li, Y., Zhao, Y., Sun, Y., Li, Y., Wang, Y., Yu, Y., Zheng, Y., Zhang, Y., Shi, Y., Xiong, Y., He, Y., Tang, Y., Piao, Y., Wang, Y., Tan, Y., Ma, Y., Liu, Y., Guo, Y., Wu, Y., Ou, Y., Zhu, Y., Wang, Y., Gong, Y., Zou, Y., He, Y., Zha, Y., Xiong, Y., Ma, Y., Yan, Y., Luo, Y., You, Y., Liu, Y., Zhou, Y., Wu, Z. F., Ren, Z. Z., Ren, Z., Sha, Z., Fu, Z., Xu, Z., Huang, Z., Zhang, Z., Xie, Z., Zhang, Z., Hao, Z., Gou, Z., Ma, Z., Yan, Z., Shao, Z., Xu, Z., Wu, Z., Zhang, Z., Li, Z., Gu, Z., Zhu, Z., Liu, Z., Li, Z., Xie, Z., Song, Z., Gao, Z., and Pan, Z. Deepseek-v3 technical report, 2025. URL <https://arxiv.org/abs/2412.19437>.
- Fu, W., Gao, J., Shen, X., Zhu, C., Mei, Z., He, C., Xu, S., Wei, G., Mei, J., Wang, J., Yang, T., Yuan, B., and Wu, Y. Areal: A large-scale asynchronous reinforcement learning system for language reasoning, 2025. URL <https://arxiv.org/abs/2505.24298>.
- He, B. [perf] weight sync optimization in colocate mode, slime PR #132. <https://github.com/THUDM/slime/issues/132>, 2025. Accessed: 2025-10-14.
- He, B., Zhu, Z., and Li, J. Efficient rl training - optimizing weight sync in slime. <https://hebiao064.github.io/rl-weight-sync>, 2025. Accessed: 2025-10-14.
- Hu, J., Wu, X., Shen, W., Liu, J. K., Zhu, Z., Wang, W., Jiang, S., Wang, H., Chen, H., Chen, B., Fang, W., Xi- anyu, Cao, Y., Xu, H., and Liu, Y. Openrlhf: An easy-to-use, scalable and high-performance rlhf framework, 2025a. URL <https://arxiv.org/abs/2405.11143>.
- Hu, Z., Shen, S., Bonato, T., Jeaugey, S., Alexander, C., Spada, E., Dinan, J., Hammond, J., and Hoefler, T. Demystifying NCCL: An in-depth analysis of GPU communication protocols and algorithms, 2025b. URL <https://arxiv.org/abs/2507.04786>.
- Huang, G., Chadha, P., Kong, T., Gao, W., and Li, Z. NeMo-RL: Journey of optimizing weight transfer in large moe models by 10x. <https://github.com/NVIDIA-NeMo/RL/discussions/1189>, 2025. Accessed: 2025-10-14.
- Kalia, A., Kaminsky, M., and Andersen, D. G. Design guidelines for high performance RDMA systems. In Gulati, A. and Weatherspoon, H. (eds.), *Proceedings of the 2016 USENIX Annual Technical Conference, USENIX ATC 2016, Denver, CO, USA, June 22-24, 2016*, pp. 437–450. USENIX Association, 2016. URL <https://www.usenix.org/conference/atc16/technical-sessions/presentation/kalia>.
- Kimi Team, Bai, Y., Bao, Y., Chen, G., Chen, J., Chen, N., Chen, R., Chen, Y., Chen, Y., Chen, Y., Chen, Z., Cui, J., Ding, H., Dong, M., Du, A., Du, C., Du, D., Du, Y., Fan, Y., Feng, Y., Fu, K., Gao, B., Gao, H., Gao, P., Gao, T., Gu, X., Guan, L., Guo, H., Guo, J., Hu, H., Hao, X., He, T., He, W., He, W., Hong, C., Hu, Y., Hu, Z., Huang, W., Huang, Z., Huang, Z., Jiang, T., Jiang, Z., Jin, X., Kang, Y., Lai, G., Li, C., Li, F., Li, H., Li, M., Li, W., Li, Y., Li, Y., Li, Z., Li, Z., Lin, H., Lin, X., Lin, Z., Liu, C., Liu, C.,

- Liu, H., Liu, J., Liu, J., Liu, L., Liu, S., Liu, T. Y., Liu, T., Liu, W., Liu, Y., Liu, Y., Liu, Y., Liu, Y., Liu, Z., Lu, E., Lu, L., Ma, S., Ma, X., Ma, Y., Mao, S., Mei, J., Men, X., Miao, Y., Pan, S., Peng, Y., Qin, R., Qu, B., Shang, Z., Shi, L., Shi, S., Song, F., Su, J., Su, Z., Sun, X., Sung, F., Tang, H., Tao, J., Teng, Q., Wang, C., Wang, D., Wang, F., Wang, H., Wang, J., Wang, J., Wang, J., Wang, S., Wang, S., Wang, Y., Wang, Y., Wang, Y., Wang, Y., Wang, Y., Wang, Z., Wang, Z., Wang, Z., Wei, C., Wei, Q., Wu, W., Wu, X., Wu, Y., Xiao, C., Xie, X., Xiong, W., Xu, B., Xu, J., Xu, J., Xu, L. H., Xu, L., Xu, S., Xu, W., Xu, X., Xu, Y., Xu, Z., Yan, J., Yan, Y., Yang, X., Yang, Y., Yang, Z., Yang, Z., Yang, Z., Yao, H., Yao, X., Ye, W., Ye, Z., Yin, B., Yu, L., Yuan, E., Yuan, H., Yuan, M., Zhan, H., Zhang, D., Zhang, H., Zhang, W., Zhang, X., Zhang, Y., Zhang, Y., Zhang, Y., Zhang, Y., Zhang, Y., Zhang, Y., Zhang, Z., Zhao, H., Zhao, Y., Zheng, H., Zheng, S., Zhou, J., Zhou, X., Zhou, Z., Zhu, Z., Zhuang, W., and Zu, X. Kimi k2: Open agentic intelligence, 2025. URL <https://arxiv.org/abs/2507.20534>.
- Kwon, W., Li, Z., Zhuang, S., Sheng, Y., Zheng, L., Yu, C. H., Gonzalez, J., Zhang, H., and Stoica, I. Efficient memory management for large language model serving with pagedattention. In Flinn, J., Seltzer, M. I., Druschel, P., Kaufmann, A., and Mace, J. (eds.), *Proceedings of the 29th Symposium on Operating Systems Principles, SOSP 2023, Koblenz, Germany, October 23-26, 2023*, pp. 611–626. ACM, 2023. doi: 10.1145/3600006.3613165. URL <https://doi.org/10.1145/3600006.3613165>.
- Langer, A., Howell, S., Potluri, S., Dinan, J., and Kraus, J. Dynamic symmetric heap allocation in NVSHMEM. In *OpenSHMEM and Related Technologies. OpenSHMEM in the Era of Exascale and Smart Networks: 8th Workshop on OpenSHMEM and Related Technologies, OpenSHMEM 2021, Virtual Event, September 14–16, 2021, Revised Selected Papers*, pp. 187–198, Berlin, Heidelberg, 2021. Springer-Verlag. ISBN 978-3-031-04887-6. doi: 10.1007/978-3-031-04888-3_12. URL https://doi.org/10.1007/978-3-031-04888-3_12.
- Li, S., Zhao, Y., Varma, R., Salpekar, O., Noordhuis, P., Li, T., Paszke, A., Smith, J., Vaughan, B., Damania, P., and Chintala, S. PyTorch Distributed: Experiences on accelerating data parallel training. *Proc. VLDB Endow.*, 13(12):3005–3018, 2020. doi: 10.14778/3415478.3415530. URL <http://www.vldb.org/pvldb/vol13/p3005-li.pdf>.
- Li, Z. feat: refit refactoring with zmq and overlapping, NeMo-RL PR #1267. <https://github.com/NVIDIA-NeMo/RL/pull/1267>, 2025. Accessed: 2025-10-14.
- Licker, N., Hu, K., Zaytsev, V., and Chen, L. pplx-kernels: Perplexity MoE kernels. <https://github.com/perplexityai/pplx-kernels>, 2025.
- Liu, A., Feng, B., Wang, B., Wang, B., Liu, B., Zhao, C., Dengr, C., Ruan, C., Dai, D., Guo, D., et al. Deepseek-v2: A strong, economical, and efficient mixture-of-experts language model. *arXiv preprint arXiv:2405.04434*, 2024.
- Mao, Z., Zhou, Y., Zhang, Y., Cui, C., Chen, Z., and Xu, Z. Previewing UCCL-EP: Flexible and efficient expert parallelism for cloud and beyond. <https://uccl-project.github.io/posts/uccl-ep/>, 2025.
- Mei, Z., Fu, W., Li, K., Wang, G., Zhang, H., and Wu, Y. Real: Efficient rlhf training of large language models with parameter reallocation. In *Proceedings of the Eighth Conference on Machine Learning and Systems, MLSys 2025, Santa Clara, CA, USA, May 12-15, 2025*. mlsys.org, 2025.
- Moonshot AI. How Kimi K2 achieves efficient RL parameter updates. <https://moonshotai.github.io/checkpoint-engine/>, 2025. Accessed: 2025-10-14.
- MPI Forum. *MPI: A Message-Passing Interface Standard Version 5.0*, June 2025. URL <https://www.mpi-forum.org/docs/mpi-5.0/mpi50-report.pdf>.
- NVIDIA. GPUDirect RDMA, 2012. URL <https://docs.nvidia.com/cuda/gpudirect-rdma/>.
- NVIDIA. NVIDIA collective communication library (NCCL), 2015. URL <https://developer.nvidia.com/nccl>.
- NVIDIA. TensorRT-LLM. <https://github.com/ai-dynamo/nixl>, 2023.
- NVIDIA. NIXL: NVIDIA inference xfer library. <https://github.com/ai-dynamo/nixl>, 2025.
- OFI WG. libfabric: Open Fabrics Interfaces (OFI), 2014. URL <https://github.com/ofiwg/libfabric>.
- Patel, P., Choukse, E., Zhang, C., Shah, A., Goiri, Í., Maleki, S., and Bianchini, R. Splitwise: Efficient generative LLM inference using phase splitting. In *51st ACM/IEEE Annual International Symposium on Computer Architecture, ISCA 2024, Buenos Aires, Argentina, June 29 - July 3, 2024*, pp. 118–132. IEEE, 2024. doi: 10.1109/ISCA59077.2024.00019. URL <https://doi.org/10.1109/ISCA59077.2024.00019>.
- Perplexity AI. Lower latency and higher throughput with multi-node DeepSeek deployment. <https://research.perplexity.ai/articles/>

- lower-latency-and-higher-throughput-with-multi-
2025.
- Qin, R., Li, Z., He, W., Cui, J., Ren, F., Zhang, M., Wu, Y., Zheng, W., and Xu, X. Mooncake: Trading more storage for less computation — a KVCache-centric architecture for serving LLM chatbot. In *23rd USENIX Conference on File and Storage Technologies (FAST 25)*, pp. 155–170, Santa Clara, CA, February 2025. USENIX Association. ISBN 978-1-939133-45-8. URL <https://www.usenix.org/conference/fast25/presentation/qin>.
- Reda, W., Canini, M., Kostic, D., and Peter, S. RDMA is turing complete, we just did not know it yet! In Phanishayee, A. and Sekar, V. (eds.), *19th USENIX Symposium on Networked Systems Design and Implementation, NSDI 2022, Renton, WA, USA, April 4-6, 2022*, pp. 71–85. USENIX Association, 2022. URL <https://www.usenix.org/conference/nsdi22/presentation/reda>.
- Sergeev, A. and Balso, M. D. Horovod: fast and easy distributed deep learning in tensorflow, 2018. URL <https://arxiv.org/abs/1802.05799>.
- SGLang. Deploying DeepSeek with PD disaggregation and large-scale expert parallelism on 96 H100 GPUs. <https://lmsys.org/blog/2025-05-05-large-scale-ep/>, 2025.
- Shah, A., Jangda, A., Li, B., Rocha, C., Hwang, C., Jose, J., Musuvathi, M., Saarikivi, O., Cheng, P., Zhou, Q., Dathathri, R., Maleki, S., and Yang, Z. Msccl++: Rethinking gpu communication abstractions for cutting-edge ai applications, 2025. URL <https://arxiv.org/abs/2504.09014>.
- Shalev, L., Ayoub, H., Bshara, N., and Sabbag, E. A cloud-optimized transport protocol for elastic and scalable HPC. *IEEE Micro*, 40(6):67–73, 2020. doi: 10.1109/MM.2020.3016891. URL <https://doi.org/10.1109/MM.2020.3016891>.
- Shamis, P., Venkata, M. G., Lopez, M. G., Baker, M. B., Hernandez, O., Itigin, Y., Dubman, M., Shainer, G., Graham, R. L., Liss, L., et al. UCX: an open source framework for HPC network APIs and beyond. In *2015 IEEE 23rd Annual Symposium on High-Performance Interconnects*, pp. 40–43. IEEE, 2015.
- Shazeer, N., Mirhoseini, A., Maziarz, K., Davis, A., Le, Q. V., Hinton, G. E., and Dean, J. Outrageously large neural networks: The sparsely-gated mixture-of-experts layer. In *5th International Conference on Learning Representations, ICLR 2017, Toulon, France, April 24-26, 2017, Conference Track Proceedings*. OpenReview.net, 2017. URL <https://openreview.net/forum?id=B1ckMDqlg>.
- Sheng, G., Zhang, G., Yao, Z., Wu, X., Zhang, W., Zhang, R., Peng, Y., Lin, H., and Wu, C. Hybridflow: A flexible and efficient rlhf framework. *arXiv preprint arXiv:2409.19256*, 2024.
- Shi, R., Potluri, S., Hamidouche, K., Perkins, J. L., Li, M., Rossetti, D., and Panda, D. K. Designing efficient small message transfer mechanism for inter-node MPI communication on InfiniBand GPU clusters. In *21st International Conference on High Performance Computing, HiPC 2014, Goa, India, December 17-20, 2014*, pp. 1–10. IEEE Computer Society, 2014. doi: 10.1109/HIPC.2014.7116873. URL <https://doi.org/10.1109/HiPC.2014.7116873>.
- Shoeybi, M., Patwary, M., Puri, R., LeGresley, P., Casper, J., and Catanzaro, B. Megatron-LM: Training multi-billion parameter language models using model parallelism, 2020. URL <https://arxiv.org/abs/1909.08053>.
- Singhvi, A., Dukkipati, N., Chandra, P., Wassel, H. M. G., Sharma, N. K., Rebello, A., Schuh, H., Kumar, P., Montazeri, B., Bansod, N., Thomas, S., Cho, I., Seibert, H. L., Wu, B., Yang, R., Li, Y., Huang, K., Yin, Q., Agarwal, A., Vaduvatha, S., Wang, W., Moshref, M., Ji, T., Wetherall, D., and Vahdat, A. Falcon: A reliable, low latency hardware transport. In Curado, M., Rothenberg, C. E., Porter, G., and Kandula, S. (eds.), *Proceedings of the ACM SIGCOMM 2025 Conference, SIGCOMM 2025, São Francisco Convent, Coimbra, Portugal, September 8-11, 2025*, pp. 248–263. ACM, 2025. doi: 10.1145/3718958.3754353. URL <https://doi.org/10.1145/3718958.3754353>.
- vLLM. Dual batch overlap. <https://github.com/vllm-project/vllm/blob/v0.13.0/docs/design/dbo.md>, 2025.
- Wu, B., Wang, S., Tang, Y., Ding, J., Helenowski, E., Tan, L., Xu, T., Gowda, T., Chen, Z., Zhu, C., Tang, X., Qian, Y., Zhu, B., and Hou, R. LlamaRL: A distributed asynchronous reinforcement learning framework for efficient large-scale LLM training, 2025. URL <https://arxiv.org/abs/2505.24034>.
- Yang, A., Li, A., Yang, B., Zhang, B., Hui, B., Zheng, B., Yu, B., Gao, C., Huang, C., Lv, C., Zheng, C., Liu, D., Zhou, F., Huang, F., Hu, F., Ge, H., Wei, H., Lin, H., Tang, J., Yang, J., Tu, J., Zhang, J., Yang, J., Yang, J., Zhou, J., Zhou, J., Lin, J., Dang, K., Bao, K., Yang, K., Yu, L., Deng, L., Li, M., Xue, M., Li, M., Zhang, P., Wang, P., Zhu, Q., Men, R., Gao, R., Liu, S., Luo, S., Li, T., Tang, T., Yin, W., Ren, X., Wang, X., Zhang, X., Ren, X., Fan, Y., Su, Y., Zhang, Y., Zhang, Y., Wan, Y., Liu, Y., Wang, Z., Cui, Z., Zhang, Z., Zhou, Z., and Qiu, Z. Qwen3 technical report, 2025. URL <https://arxiv.org/abs/2505.09388>.

- Ye, Z., Chen, L., Lai, R., Lin, W., Zhang, Y., Wang, S., Chen, T., Kasikci, B., Grover, V., Krishnamurthy, A., and Ceze, L. FlashInfer: Efficient and customizable attention engine for LLM inference serving, 2025. URL <https://arxiv.org/abs/2501.01005>.
- Zhang, S., Zheng, N., Lin, H., Jiang, Z., Bao, W., Jiang, C., Hou, Q., Cui, W., Zheng, S., Chang, L.-W., Chen, Q., and Liu, X. COMET: Fine-grained computation-communication overlapping for mixture-of-experts. In *Eighth Conference on Machine Learning and Systems*, 2025. URL <https://openreview.net/forum?id=fGgQS5VW09>.
- Zhao, C., Zhou, S., Zhang, L., Deng, C., Xu, Z., Liu, Y., Yu, K., Li, J., and Zhao, L. DeepEP: an efficient expert-parallel communication library. <https://github.com/deepseek-ai/DeepEP>, 2025.
- Zhao, Y., Gu, A., Varma, R., Luo, L., Huang, C.-C., Xu, M., Wright, L., Shojanazeri, H., Ott, M., Shleifer, S., Desmaison, A., Balioglu, C., Damania, P., Nguyen, B., Chauhan, G., Hao, Y., Mathews, A., and Li, S. PyTorch FSDP: Experiences on scaling fully sharded data parallel. *Proc. VLDB Endow.*, 16(12):3848–3860, August 2023. ISSN 2150-8097. doi: 10.14778/3611540.3611569. URL <https://doi.org/10.14778/3611540.3611569>.
- Zheng, L., Yin, L., Xie, Z., Sun, C., Huang, J., Yu, C. H., Cao, S., Kozyrakis, C., Stoica, I., Gonzalez, J. E., Barrett, C. W., and Sheng, Y. Sglang: Efficient execution of structured language model programs. In Globersons, A., Mackey, L., Belgrave, D., Fan, A., Paquet, U., Tomczak, J. M., and Zhang, C. (eds.), *Advances in Neural Information Processing Systems 38: Annual Conference on Neural Information Processing Systems 2024, NeurIPS 2024, Vancouver, BC, Canada, December 10 - 15, 2024*, 2024. URL http://papers.nips.cc/paper_files/paper/2024/hash/724be4472168f31ba1c9ac630f15dec8-Abstract-Conference.html.
- Zheng, S., Bao, W., Hou, Q., Zheng, X., Fang, J., Huang, C., Li, T., Duanmu, H., Chen, R., Xu, R., Guo, Y., Zheng, N., Jiang, Z., Di, X., Wang, D., Ye, J., Lin, H., Chang, L.-W., Lu, L., Liang, Y., Zhai, J., and Liu, X. Triton-distributed: Programming overlapping kernels on distributed ai systems with the triton compiler, 2025a. URL <https://arxiv.org/abs/2504.19442>.
- Zheng, S., Fang, J., Zheng, X., Hou, Q., Bao, W., Zheng, N., Jiang, Z., Wang, D., Ye, J., Lin, H., et al. Tilelink: Generating efficient compute-communication overlapping kernels using tile-centric primitives. *arXiv preprint arXiv:2503.20313*, 2025b.
- Zhong, Y., Liu, S., Chen, J., Hu, J., Zhu, Y., Liu, X., Jin, X., and Zhang, H. Distserve: Disaggregating prefill and decoding for goodput-optimized large language model serving. In Gavrilovska, A. and Terry, D. B. (eds.), *18th USENIX Symposium on Operating Systems Design and Implementation, OSDI 2024, Santa Clara, CA, USA, July 10-12, 2024*, pp. 193–210. USENIX Association, 2024. URL <https://www.usenix.org/conference/osdi24/presentation/zhong-yinmin>.
- Zhou, Y., Chen, Z., Mao, Z., Lao, C., Yang, S., Kannan, P. G., Gao, J., Zhao, Y., Wu, Y., You, K., Ren, F., Xu, Z., Raiciu, C., and Stoica, I. An extensible software transport layer for gpu networking, 2025. URL <https://arxiv.org/abs/2504.17307>.
- Zhu, Z., Xie, C., Lv, X., and slime Contributors. slime: An llm post-training framework for rl scaling. <https://github.com/THUDM/slime>, 2025. GitHub repository. Corresponding author: Xin Lv.

A KVCACHE TRANSFER PSEUDOCODE

```
struct DispatchReq {
    input_ids: Vec<u32>,
    decoder_addr: NetAddr, imm: u32,
    kv_desc: MrDesc, pages: Vec<u32>,
    tail_desc: MrDesc, tail_idx: u32,
}
```

Figure 13. Message sent from decoder to prefiller via SEND/RECV.

```
def decoder_engine(req: Request, prefiller: NetAddr):
    # Allocate from GPU memory pool
    page_indices: list[int] = alloc_pages(req)
    tail_idx: int = alloc_tail()
    # Set up ImmCounter callback
    imm = alloc_imm()
    imm_count = len(page_indices) * n_layers + 1
    ev = Event()
    te.expect_imm_count(imm, imm_count, lambda: ev.set())
    # Dispatch to prefiller via RDMA SEND
    te.submit_send(prefiller, serialize(DispatchReq(...)))
    # Start decode once received all WRITES from Prefiller
    ev.wait()
    process_tail(tail[tail_idx])
    free_imm(imm); free_tail(tail_idx)
    auto_regressive_decode(...)
    free_pages(...)
```

Figure 14. Decoder workflow

This section provides pseudocode for the disaggregated Kv-Cache transfer workflow described in Section 4, using the *TransferEngine* API from Figure 2. For clarity, the pseudocode uses a synchronous, blocking style; in practice, all operations are asynchronous tasks on a Tokio event loop. *Tail context* refers to auxiliary GPU tensors transferred from prefiller to decoder beyond the KvCache—in this example, the output logits. The specific contents are inference-engine-dependent, but the transfer pattern is the same.

For brevity, the pseudocode omits: (1) sharding and replication of KV heads for tensor parallelism and Multi-head Latent Attention (MLA); (2) support for multiple KvCache buffers (e.g., separate key and value buffers); (3) chunked prefill, which does not change the total number of transferred pages or the expected `imm_count` but requires additional bookkeeping; (4) prefix-cache reuse, where pages already present on the decoder need not be transferred from the prefiller; (5) stride and offset computations for WRITES.

Figure 13 shows the message sent from decoder to prefiller. The decoder includes its RDMA memory descriptors (`kv_desc`, `tail_desc`) and page indices so the prefiller can WRITE directly into the decoder’s GPU memory.

Figure 14 shows the decoder workflow. The decoder pre-registers an `IMMCOUNTER` with the expected number of `WRITEIMM` completions before dispatching, so no explicit completion message is needed from the prefiller.

Figure 15 shows the prefiller workflow. UVM watcher overlaps KvCache transfer with computation. After each layer’s attention, the GPU increments a UVM counter via

```
def prefiller_init():
    te.submit_recv(MAX_LEN, MAX_RECV,
        lambda msg: prefiller_engine(deserialize(msg)))

def prefiller_engine(req: DispatchReq):
    # Allocate from GPU memory pool
    page_indices: list[int] = alloc_pages(req)
    tail_idx: int = alloc_tail()
    # Set up UvmWatcher (CUDA graph compatible)
    cnt_done = 0
    def uvm_cb(old: int, new: int):
        for layer in range(old, new):
            # RDMA WRITE pages to decoder
            te.submit_paged_writes(...,
                on_done=lambda: cnt_done += n_pages)
    watcher_ptr = te.alloc_uvm_watcher(uvm_cb)
    # Model forward
    x = embed(req.input_ids)
    for i in range(num_layers):
        x = self_attn(x)
        scalar_inc_(watcher_ptr)
        x = mlp(x)
    x = lm_head(x)
    tail[tail_idx].copy_(x) # Or other tail context
    # RDMA WRITE tail context to decoder
    tail[tail_idx].synchronize()
    te.submit_single_write(...,
        on_done=lambda: cnt_done += 1)
    # Wait until all RDMA WRITES are done
    while cnt_done != n_pages * n_layers + 1:
        sleep(0)
    free_tail(tail_idx); free_pages(page_indices)
```

Figure 15. Prefiller workflow

`scalar_inc_`; the CPU-side callback fires and submits `WRITEIMM` for that layer while the next layer computes.

B RL WEIGHT TRANSFER PSEUDOCODE

```
@ray.remote
class TrainingWorker:
    def param_meta(self) -> dict[str, ParamMeta]: ...
    def set_routing(self, route: RoutingTable) -> None: ...
    def transfer_weights(self) -> None: ...

@ray.remote
class RolloutWorker:
    def param_meta(self) -> dict[str, ParamMeta]: ...
    def memory_regions(self) -> list[MemoryRegion]: ...

def controller_main() -> None:
    # Init and gather metadata
    trainers: list[TrainingWorker] = ...
    rollouts: list[Rolloutworker] = ...
    t_params = ray.get([x.param_meta() for x in trainers])
    r_params = ray.get([x.param_meta() for x in rollouts])
    r_mrs = ray.get([x.memory_regions() for x in rollouts])
    # Compute and set weight transfer routing
    route = compute_routing(t_params, r_params, r_mrs)
    ray.get([x.set_routing(route) for x in trainers])
    # Training loop
    while training_not_done:
        train()
        ray.get([x.transfer_weights() for x in trainers])
        rollout()
```

Figure 16. RL training and weight update workflow

Figure 16 shows the RL weight transfer workflow described in Section 5. The controller gathers parameter metadata and memory region descriptors from all workers, computes a static routing table that maps each training GPU’s parameters to the target inference GPU memory regions, and broadcasts the routing to training workers. At each training step, training workers execute the weight transfer using the pre-computed routing, without re-planning or coordination.